Energy 58 (2013) 376–383

Contents lists available at SciVerse ScienceDirect

Energy

journal homepage: www.elsevier.com/locate/energy

Effect of residence time on chemical and structural properties of hydrochar obtained by hydrothermal carbonization of water hyacinth

Ying Gao, Xianhua Wang*, Jun Wang, Xiangpeng Li, Jianjun Cheng, Haiping Yang, Hanping Chen

State Key Laboratory of Coal Combustion, Huazhong University of Science and Technology, 1037 Luoyu Road, 430074 Wuhan, PR China

ARTICLE INFO

Article history:
Received 18 January 2013
Received in revised form
3 June 2013
Accepted 11 June 2013
Available online 10 July 2013

Keywords:
Water hyacinth
Hydrothermal
Carbonation
Hydrochar

ABSTRACT

Hydrothermal carbonization of water hyacinth was experimentally conducted in the range of 30 min to 24 h at 240 °C, chemical and structural properties of hydrochar products were investigated. Oxygen/carbon ratio, and hydrogen/carbon ratio in all hydrochar products were 0.19–0.45, and 0.94 to 1.51. Higher heating value of hydrochar products was 16.83 MJ/kg to 20.63 MJ/kg. Residence time had little effect on the chemical properties of hydrochar samples after 4 h. When the residence time was more than 4 h, hydrochar products exhibited almost the same pyrolysis behavior under TGA (thermogravimetric analysis). Hydrochar developed better structural characterization as time increased. The formation of microspheres on the surface of hydrochar was discussed, and transformation of cellulose and hemicellulose should be the reaction for microsphere production.

1. Introduction

Progress comes with an increasing utilization of environmental resources by humans, development of industries, and a high concentration of urban population; thus, a large amount of wastewater from industries and domestic sewage are not properly discharged into water bodies. Eutrophication then takes place, induced by wastewater increasing the concentration of oxygen consumption materials (nitrogen, phosphorus and organic pollutants) in water bodies [1,2]. Aquatic plants, such as water hyacinth, are directly influenced by water eutrophication [3,4]. Water hyacinth is a harmful plant with flourishing roots and recommends to be one of the world's worst aquatic plants [5]. And water hyacinth would clog river course, reservoir and channel. A large amount of man power and money have been spent on water hyacinth; however, these aquatic plants can still not be completely eliminated [5,6]. The task of determining how water hyacinth can be treated as biomass resource has not been carried out. Therefore, using these aquatic plants as biomass resource is urgent.

In recent years, HT (hydrothermal technology) has been the research hotspot for highly efficient conversion technology. HT process mixes biomass and water to produce gas, liquid, and solid products without pretreatment at certain pressure and temperature [7]. Moisture content for biomass has no limit during the HT process. Solubility and crystallization take place in subcritical and supercritical conditions, thus avoiding problems such as agglomeration in traditional pyrolysis. HT condition directly determines composition and proportion of the target product [8]. HT can be divided into HTC (hydrothermal carbonization), HTL (hydrothermal liquefaction), and HTG (hydrothermal gasification) according to the target products. HTC is usually performed at a temperature of 180 °C–250 °C and a pressure of 14 bar–276 bar; the process may last 1 min to several hours under inert atmosphere [9–11]. It is a most effective process to convert lignocellulosic materials into hydrochar, condensable organic liquids, and non-condensable gases by hot compressed water.

Water hyacinth belongs to cellulosic biomass; organic components include proteins, nitrogen free extract (starch, sugars, and pectin), and lipoid materials. Two prominent characteristics of water hyacinth are compared with those of agricultural wastes. First, water content of water hyacinth is up to 95%; the drying process increases cost of utilization and decreases efficiency. Second, ash content of water hyacinth is about 17%–35% [12]; alkali metals in the ash induces several problems, such as particles agglomerated in pyrolysis and heated surface deposition. A number

* Corresponding author. Tel.: +86 (0)27 87542417x8211; fax: +86 (0)27 87545526.
E-mail addresses: gstshwgy@163.com (Y. Gao), wxhwhhy@sina.com, BoYuyubocumt@163.com (X. Wang), troywang@126.com (J. Wang), lixiangpeng15@126.com (X. Li), hbchengjianjun@163.com (J. Cheng), yhping2002@163.com (H. Yang), hp.chen@163.com (H. Chen).

0360-5442/$ – see front matter © 2013 Elsevier Ltd. All rights reserved.
http://dx.doi.org/10.1016/j.energy.2013.06.023

of technological options are available as renewable fuel and chemical feedstock for water hyacinth [13–15]. These technologies are focused on hydrolysis [16,17], fermentation [18,19], HTL [20–22] and HTG [23]; and are optimized to improve quality and increase quantity of target products. Bioconversion in the production of biogas from water hyacinth has been demonstrated in recent years [24]. Elliott et al. found that high-moisture biomass feedstock can be a source of useful liquid fuel products. Yield of water hyacinth oil was 26% [25]. The high cost and technological level necessary for carbonization make this process an unfavorable alternative to producing charcoal from water hyacinth. Gao et al. studied the hydrothermal carbonation of cellulose, xylan, water hyacinth and rice straw at 240 °C for 4 h. The hydrochar yield of the water hyacinth was the highest, and the hydrochar was composed of carbon microspheres in the form of core–shell [26]. However, there have been very few studies about the properties of hydrochar from hydrothermal carbonation of water hyacinth at different residence time.

The present paper studied the effect of hydrothermal residence time on the characteristics of hydrochar products. The investigation focused on the analysis of chemical and structural features of hydrochar by elemental analysis, TGA (thermogravimetric analysis), FTIR (Fourier transform infrared), XRD (X-ray diffraction), XPS (X-ray photoelectron spectroscopy), SEM (scanning electron microscopy), and TEM (transmission electron microscopy).

2. Materials and methods

2.1. Samples

Water hyacinth was gathered from a farm in Xuzhou, southeast China. Biomass materials were crushed by a high-speed rotary cutting mill and screened; only particles smaller than 80 mesh were used and dried at 105 °C until the weight was constant.

2.2. Apparatus and procedure

Fig. 1 is the schematic diagram of experimental apparatus. All experiments were carried out in a 500 mL autoclave of 316 L stainless steel. The autoclave can be operated at a maximum temperature of 600 °C and maximum pressure of 40 MPa. The autoclave was warmed by an electric heater. Temperature was measured by a K-thermocouple and controlled at ±5 °C. Pressure was measured at an accuracy of 2%.

For each test, 6 g of water hyacinth and 100 g of deionized water were placed in the autoclave and sealed. The reactor was purged using argon. Then, the experimental setup was heated from ambient temperature to 240 °C. Retention time was 30 min to 24 h. All experiments were repeated three times and averaged using a set of numbers.

Temperature profiles of the experiments are shown in reference [27]. After the desired temperature and reaction time have reached, the autoclave was cooled by internal cooling U-loop and external fan. Reactor temperature fell below 90 °C in less than 15 min for each experiment. Then, temperature dropped to room temperature, and the remaining gas was vented. The solid liquid mixture from the autoclave was collected and separated. Water-insoluble fractions, retained on the autoclave and stirring blade, were washed three times with deionized water. With the filter device, the water-soluble fraction was taken at an aqueous phase and centrifuged at 4000 rpm to remove suspended solids. Solids, which are insoluble in water, were dried at 105 °C. The procedure for separating products is shown in Fig. 2.

2.3. Analysis of the hydrochar products

Elemental analyses of hydrochar samples for carbon, hydrogen, and oxygen were carried out using an elementary analyzer (Vario Micro Cube, Germany).

The chemical composition of hydrochar samples was analyzed by FTIR (Bruker's VERTEX-70) and XPS (VG Multilab 2000). X-ray photoelectron spectra were obtained with a vacuum generator using MgKα radiation. XRD (PANalytical B.V, X'Pert PRO, the Netherlands) for the crystal structure of solid products was also carried out to provide more information on hydrochar samples during HTC. Ground sample was loaded into a rectangular cavity holder, and XRD was performed at 40 kV and 40 mA using Cu Kα radiation. Diffraction patterns were collected in the 2θ range of 15°–60° in steps of 0.0171° with a count time of 11.16 s.

Thermal analysis of hydrochar was carried out through TGA (NETZSCH STA 409C, Germany). A 10 mg sample was placed in a sample pan. Temperature was increased from ambient temperature to 900 °C, with a heating rate of 10 °C/min. Thermogravimetry (TG) experiments were performed under flowing purified nitrogen (99.9995%) atmosphere at a flow rate of 100 mL/min.

Hydrochar samples were analyzed by SEM (Quanta200, FEI, Holland) and TEM (Tecnai G220). TEM was operated at an acceleration potential of 200 kV. Hydrochar samples were prepared for TEM by ultrasonically suspending the powder sample in ethanol and placing a drop of the suspension on a holey carbon copper grid. After evaporation of the solvent, hydrochar samples were introduced to the TEM microscope column.

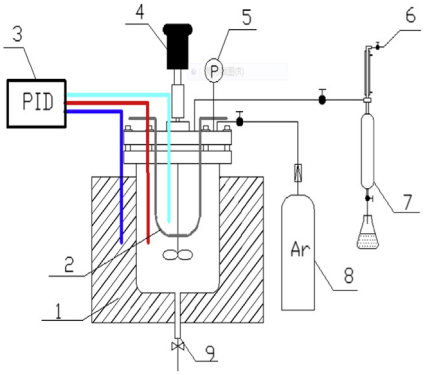

Fig. 1. Schematic diagram of experimental apparatus. 1. autoclave, 2. condensing coil, 3. temperature controller, 4. stirrer, 5. pressure gauge, 6. gas sampling, 7. liquid sampling, 8. Ar cylinder, 9. drain valve.

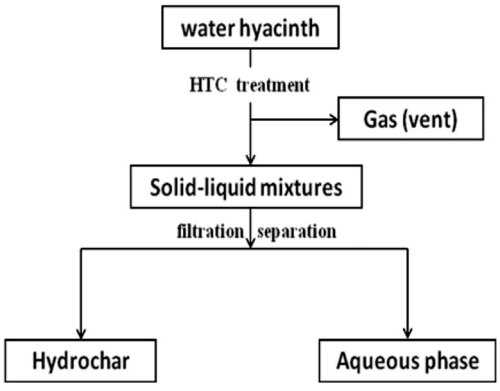

Fig. 2. Separation of products after HTC.

Table 1
Proximate, ultimate and component analyses (wt.%) of water hyacinth.

	Water hyacinth
Ultimate analysis (wt.%, dry basis)	
C	29.75
H	5.41
N	2.03
S	0.33
O[a]	24.7
Proximate analysis (wt.%)	
M_{ad}	5.69
V_{ad}	49.92
FC_{ad}	6.28
A_d	38.11
Chemical analysis (wt.%)	
Cellulose	16.5
Hemicellulose	18.9
Lignin	11.6

M: moisture content; V: volatile matters; A: ash; FC: fixed carbon; ad: on air dried basis; d: on dry basis.
[a] The oxygen (O) content was determined by difference.

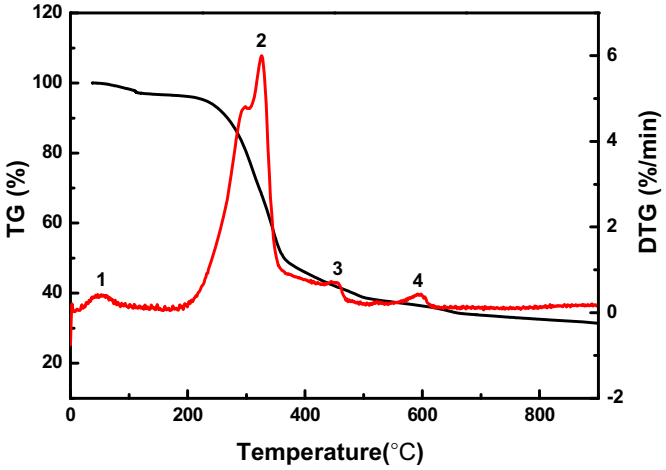

Fig. 3. TG-DTG curves of water hyacinth.

3. Results and discussion

3.1. Feedstock characterization

The proximate, ultimate and component analyses (wt.%) of water hyacinth are shown in Table 1. Besides cellulose, hemicellulose, and lignin, water hyacinth contained some fat and crude protein.

TG and derivative TG (DTG) curves of water hyacinth pyrolysis are shown in Fig. 3. Thermal degradation of water hyacinth showed four major weight loss steps. In the first weight loss step, water hyacinth corresponds to the removal of moisture in water hyacinth at a temperature range between 40 °C and 100 °C. In the second weight loss step, water hyacinth consists of the volatilization of hemicellulose and cellulose [28], at the temperature range between 200 °C and 400 °C. This stage is the maximum weight loss. The third weight loss step occurred between 440 °C and 520 °C and is related to lignin degradation. The stage beyond 520 °C is associated to the formation of char and several inorganic matter [29]. After the major weight loss, no further weight loss occurs from the temperature range of 650 °C–900 °C. The residue (38%) is the char of the water hyacinth. From XRF (X-ray fluorescence) data (Table 2), a number of inorganic materials were found in the ash of water hyacinth. Among them, silicon, phosphorus, calcium, and aluminium were highly concentrated in water hyacinth. A different amount of inorganic matter may also affect HTC results.

3.2. Chemical characteristics of hydrochar

Elemental compositions of hydrochar from water hyacinth for 30 min to 24 h are shown in Table 3. Carbon content in water hyacinth was about 30%, and carbon in hydrochar obtained from water hyacinth nearly accounted for 44%–48%. Reductions in oxygen and hydrogen content for hydrochar products compared with those of water hyacinth were observed. The reason may be that an intermolecular dehydration reaction of large molecules took place, transforming elemental hydrogen and oxygen to water. Nitrogen content of hydrochar was high, approximately 3.0%. Therefore, during the carbonization process, nitrogen took part in the emission of gases (NO_x or NH_3) and in chemical reactions. Higher heating values (HHVs) of hydrochar products were also higher than those obtained for water hyacinth because water hyacinth was lost to gaseous and liquid by-products. Calculations of HHV were performed according to Eq. (1).

$$HHV = 0.3383C + 1.422\,(H-O/8). \quad (1)$$

Furthermore, relationships among HHV, H/C (hydrogen/carbon), and O/C (oxygen/carbon) ratios of water hyacinth and hydrochar samples are shown in the Van Krevelen diagram (Fig. 4) [30,31]. H/C and O/C ratios of hydrochar produced from HTC are nearly the same with those of increased residence time. When H/C was 1.16 and O/C was 0.45, HHV of hydrochar reached the minimum; when H/C was 1.34 and O/C was 0.22, HHV of hydrochar reached the maximum. HHV first increased, and then decreased as O/C increased. Lower H/C and O/C ratios of hydrochar products compared with those of water hyacinth resulted from the evolution of H_2O and CO_2 in dehydration and decarboxylation reactions, which have several effects on the structure and functional groups of hydrochar [32]. O/C ratio was consistent with the presence of more hydroxyl, carboxylate, and carbonyl groups in HTC hydrochar. As a result, HHVs for hydrochar products were higher compared with that of water hyacinth. This may be mainly attributed to the removal of amorphous components from water hyacinth [33]. When residence time was longer than 4 h, O/C ratio obtained stability at approximately 0.2, suggesting that longer residence time has no significant effects on O/C. Because O/C ratio was similar after 4 h, hydrochar products exhibited almost the same pyrolysis behavior under TGA (Fig. 5).

TG and DTG curves for HC-30 min, HC-6 h, and HC-24 h undergoing pyrolysis in a nitrogen atmosphere at a heating rate of 10 °C/min^{-1} are shown in Fig. 5. TGA curves show that thermal decomposition of all hydrochar products included three steps.

Table 2
Inorganic properties of biomass samples (wt.% of the ash).

Sample	SiO_2	CaO	MgO	Al_2O_3	P_2O_5	SO_3	Cl	K_2O	TiO_2	Fe_2O_3
Water hyacinth	45.21	17.25	3.32	12.13	8.66	4.8	0.87	3.51	0.5	3.36

Table 3
Characteristics of water hyacinth and hydrochar (wt.%, dry basis).

	Residence time (h)						
	Original	0.5	1	2	4	6	8
C (%)	29.75	44.26	45.99	44.45	46.51	44.63	48.97
H (%)	5.41	4.29	4.22	4.05	4.09	4.12	4.63
O (%)	24.7	24.01	17.96	17.48	13.76	13.67	14.47
N (%)	2.03	2.5	2.89	2.78	2.8	2.86	2.77
Ash (%)	38.11	24.94	28.94	31.24	32.84	34.72	29.16
HHV (MJ/kg)	13.78	16.83	18.41	17.72	19.15	18.58	20.63
H/C	2.18	1.16	1.1	1.09	1.05	1.11	1.34
O/C	0.62	0.45	0.29	0.29	0.22	0.23	0.22
N/C	0.06	0.05	0.05	0.05	0.05	0.05	0.06
	Residence time (h)						
	10	12	14	16	18	20	24
C (%)	44.76	47.2	44.45	47.07	45.57	46.39	46.46
H (%)	4.29	4.3	4.11	4.46	3.75	3.6	3.98
O (%)	13.21	13.15	13.4	11.81	12.54	12.71	13.31
N (%)	3.05	2.9	3.02	2.98	3.11	2.93	3.07
Ash (%)	34.69	32.45	35.02	33.68	35.03	34.37	33.18
HHV (MJ/kg)	18.95	19.8	18.55	20.23	18.56	18.6	19.06
H/C	1.51	1.1	1.11	1.14	0.99	0.94	1.03
O/C	0.22	0.21	0.23	0.19	0.21	0.21	0.21
N/C	0.06	0.05	0.06	0.05	0.06	0.05	0.06

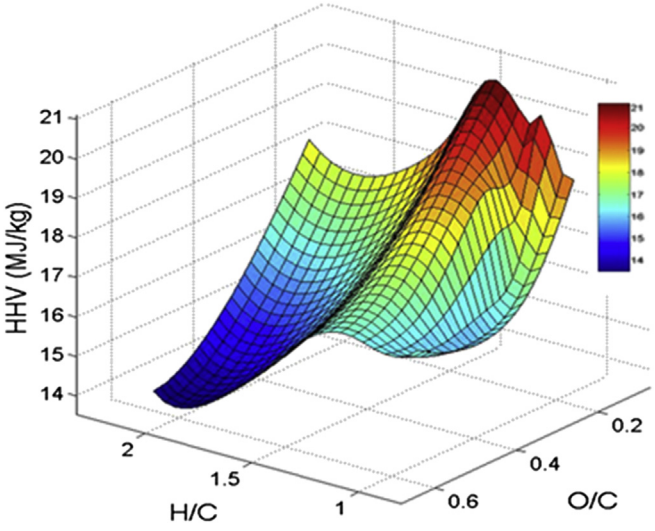

Fig. 4. Van Krevelen diagram for hydrochar samples (data from Table 3).

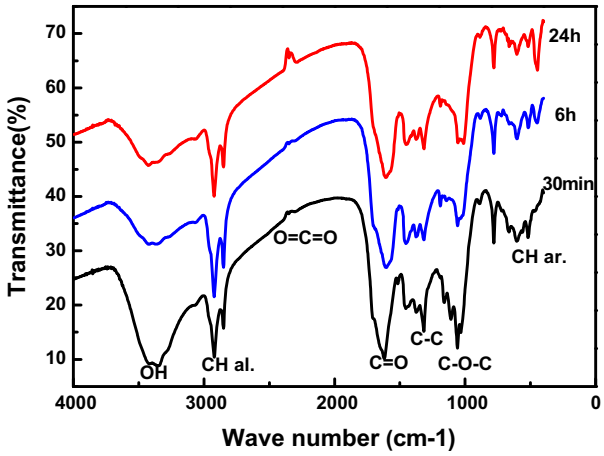

Fig. 6. FTIR spectra of the hydrochar products.

The first weight loss, which occurred at 100 °C–200 °C, was water loss. In the temperature range between 250 °C and 700 °C, a significant difference in weight loss behavior for all samples was observed. From 250 °C up to 400 °C, HC-30 min produced a distinct peak, indicating incomplete hydrolysis of cellulose and hemicellulose in hydrochar at lower residence time and rapid decomposition at a relatively lower temperature. Furthermore, hydrochar samples showed the same two overlapping peaks, which are not sharp and wide, between 400 °C and 700 °C, representing lignin residue in hydrochar and several inorganic matter [29]. Above 700 °C, weight loss was minimal, and weight remained relatively constant above 700 °C. In the untreated sample (water hyacinth), total weight loss was 69% (Fig. 2). Higher consumption was obtained in hydrochar samples: HC-30 min (61%), HC-6 h (49%), and HC-24 h (45%). The difference in the hydrochar structures and chemical properties of the HC-30 min and HC-6 h possibly account for the different behaviors observed. HC-30 min contained cellulose and hemicellulose, which were very easy to degrade to volatiles evolving out (CO, CO_2, and some hydrocarbon, etc.) at low temperatures. Different to HC-30 min, HC-6 h and HC-24 h contained only lignin residue and several inorganic matter, and the thermal stability is similar after 6 h. The FTIR results will confirm it.

FTIR spectra of hydrochar at 30 min, 6 h, and 24 h are shown in Fig. 6. Hydrochar obtained at 6 h was similar to hydrochar acquired at 24 h –OH stretching vibrations between 3200 and 3400 cm^{-1} indicate the presence of phenols and alcohols, which suggests that –OH stretching vibrations decreased with increasing carbonation residence time, which might be attributed to the dehydration of

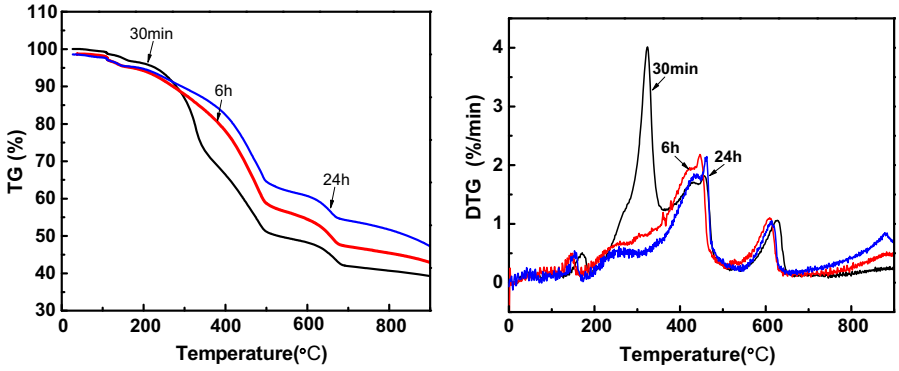

Fig. 5. TG and DTG curves for the hydrochar products.

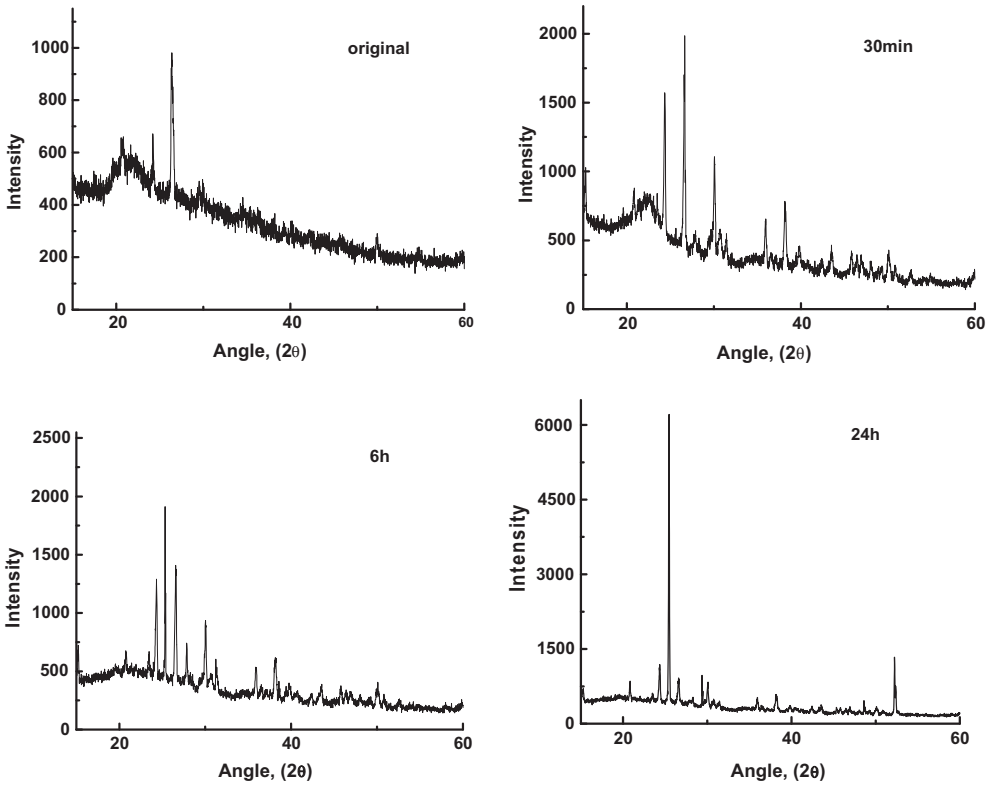

Fig. 7. XRD analysis of water hyacinth and hydrochar products.

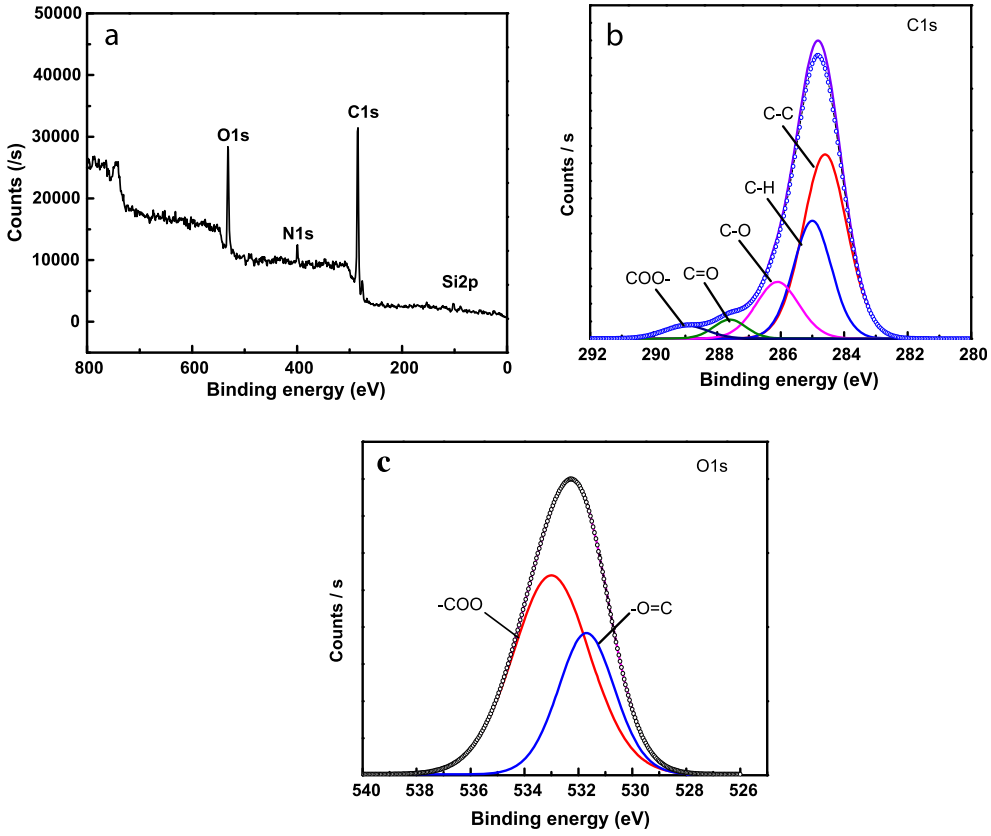

Fig. 8. (a) X-ray photoelectron spectroscopy (XPS) survey spectra of HC-24 h (b) Cls spectra of HC-24 h (c) Ols spectra of HC-24 h.

hydrochar. Absorbance peaks between 2970 cm^{-1} and 2840 cm^{-1} represent CHn stretching vibrations, which are indicative of aliphatic and aromatics. The breaking of −C−H functional groups released CH_4, C_2H_6, and C_2H_4 in gaseous products [34]. The absorbance peak at 1608 cm^{-1} and 1090 cm^{-1} represented the C═O and C−O−C groups, indicating CO_2 generation. Aromatic C−H deformation (700 cm^{-1}–900 cm^{-1}) exhibited no change with increased time. Furthermore, the peak at 1080 cm^{-1}, 804 cm^{-1}, and 460 cm^{-1} was a result of siloxane bonds (Si−O−Si). Compared with HC-6 h and HC-24 h, a big difference was found in the finger print region (1330–400 cm^{-1}) for HC-30 min. The highest IR absorbance of OH and C═O was found with HC-30 min.

Fig. 7 shows XRD patterns of hydrochar at 30 min, 6 h, and 24 h with water hyacinth. Several changes occurred in peak intensity, wherein peak intensity of hydrochar was higher than that of water hyacinth. X-ray diffractogram shows that hydrothermal processing can increase crystallinity of water hyacinth. Increase in crystallinity may be attributed to the removal of the amorphous components (i.e., lignin and hemicellulose) [35].

With the increase of residence time, XRD peaks corresponding to different phases of SiO_2 appeared, indicating that hydrochar was rich in silica, which agrees with XRF and FTIR spectra. Silica gradually transformed from an amorphous phase to a crystalline phase with increase in residence time. Crystalline has been fully formed, and better crystalline at 24 h is obtained. Sharp peaks that seemed to originate from the graphite crystalline structure appeared in hydrochar carbonized at 6 h and 24 h with high crystallization degree. XRD patterns changed gradually with an increase in residence time, possibly because of structural changes in hydrochar.

To obtain surface chemistry of hydrochar, samples can also be characterized by XPS. An example of hydrochar XPS from 24 h is given in Fig. 8a. Cls (about 285 eV) and Ols (about 531 eV) peaks were clearly resolved. Photoelectron peaks show that hydrochar consisted mainly of carbon, oxygen, nitrogen, and silica.

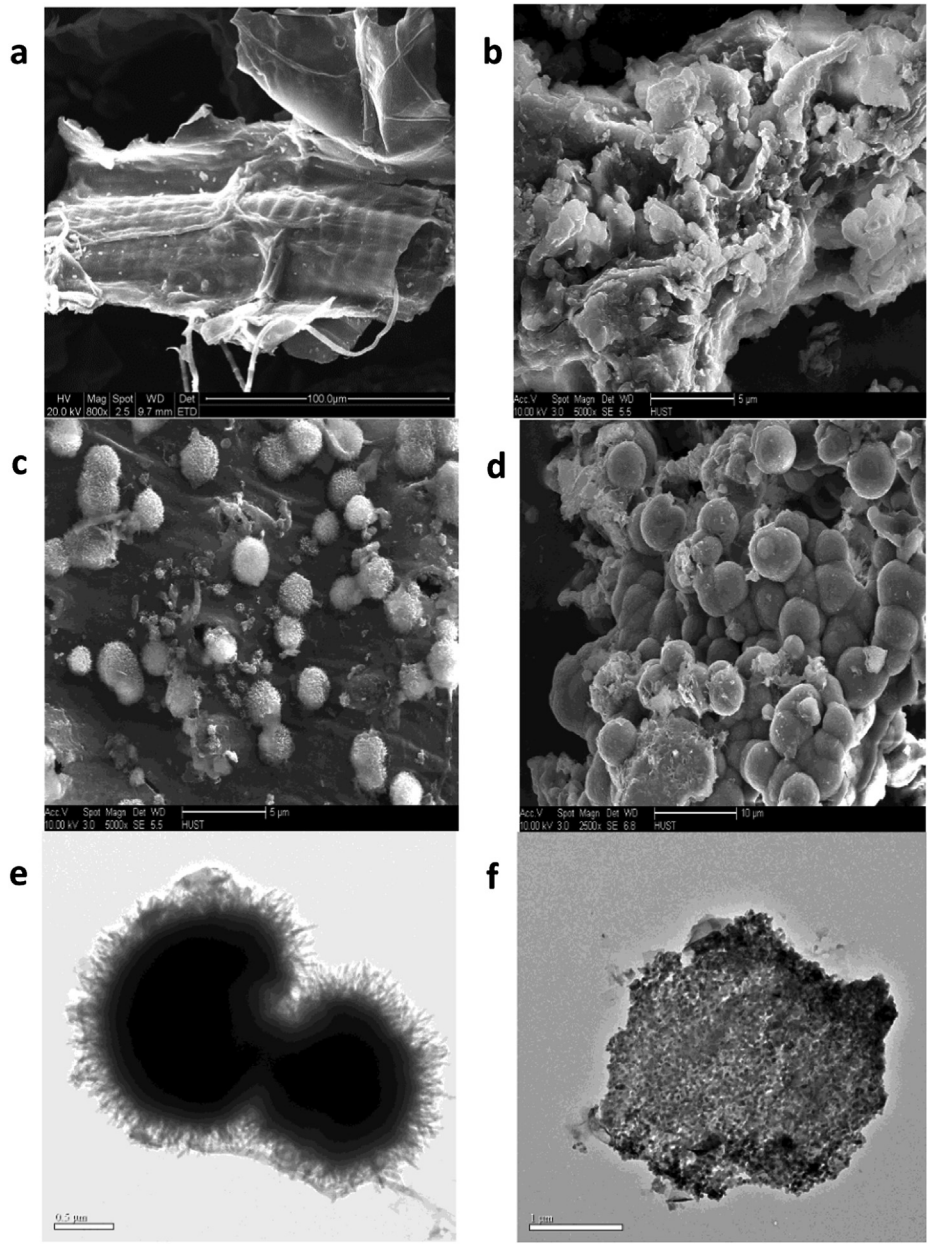

Fig. 9. SEM images of feedstock and hydrochar (a: water hyacinth, b: HC-30 min, c: HC-6 h, d: HC-24 h). TEM images of hydrochar (e: HC-6 h, f: HC-24 h).

The distribution of C and O structures can be derived from C1s and O1s spectra. Fig. 8b shows C1s spectra of hydrochar at 24 h. C–C, C–H, C–O, C=O, and COO– are the five forms of carbon present on the surface of samples. Their corresponding binding energies are 284.6, 285.3, 286.3, 287.5, and 289.0 eV, respectively [36,37]. XPS O1s results of hydrochar are shown in Fig. 8c. O1s spectra of hydrochar could both be fitted into two peaks at 531.7 eV and 533.0 eV, which were attributed to the oxygen in COO– and C=O, respectively. Overall, results indicate the presence of more oxygen-rich functional groups on the surface of hydrochar. This finding agrees with FTIR spectra.

3.3. Structural characteristics of the hydrochar

SEM micrographs of water hyacinth and hydrochar samples are presented in Fig. 9(a–d). SEM is a potential technique for studying morphology of samples after different thermal treatments. According to SEM micrographs, physical properties and surface morphology of samples changed after HTC.

From Fig. 9b, cracks and trenches can be clearly seen on the surface of HC-30 min. Small microspheres can be found on the trenches. Fig. 9c shows that HC-6 h developed microspheres and carbon microspheres seemed to be mono-dispersed on the surface with a diameter of 1 μm. However, trenches and surface cracks were not visible. Whiskers appeared on the surface of the microspheres. Fig. 9d of HC-24 h showed several aggregations of microspheres with diameters of 1 μm–5 μm, and carbon spheres were in spherical morphology, with very smooth surface without whiskers. Carbon spheres were much higher in number than those of the other two hydrochar samples. Longer residence time had a visual effect on surface morphology because cellulose and hemicellulose did not react completely at shorter residence time, according to TGA results. With an increase in residence time, cellulose and hemicellulose may be completely decomposed and can increase the number of microspheres.

For further investigation, interior textures of hydrochar were closely examined by TEM. Carbon spheres from HC-6 h exhibited a core–shell structure, and whiskers could be seen by TEM. Fig. 9f shows HC-24 h obtained from water hyacinth, which exhibited a mesoporous structure with a sponge-like morphology. This sponge-like structure is stable, providing evidence for the presence of a new stable carbon material at 24 h.

4. Conclusion

In this study, water hyacinth was converted to hydrochar by hydrothermal carbonation at temperatures of 240 °C and residence time from 30 min to 24 h. With increase in residence time, higher heating value in all hydrochar products was 16.83 MJ/kg to 20.63 MJ/kg. Hydrochar exhibited almost the same pyrolysis behavior under TGA after 4 h. Based on X-ray diffraction, water hyacinth was converted to crystalline components. Based on the SEM, TEM, FTIR, and XPS results, the SR had a core–shell structure. It contained a large number of oxygen functional groups. Longer residence time was favorable for the hydrochar production where cellulose and hemicellulose presented in the hydrochar underwent dehydration and condensation polymerization processes resulting in rich carbon microspheres. HC-24 h exhibited a stable mesoporous structure with a sponge-like morphology.

Acknowledgements

The authors wish to express the great appreciation of the financial support from Key Projects of National Fundamental Research Planning (2013CB228102)) and National Nature Science Foundation of China (51021065 and 50930006).

Appendix

HC-30 min: hydrochar from 240 °C, 30 min
HC-6 h: hydrochar from 240 °C, 6 h
HC-24 h: hydrochar from 240 °C, 24 h

References

[1] Zheng J. The performance and mechanism of removal of heavy metals from water by water hyacinth roots as a biosorbent material. Ph.D thesis 2010.
[2] Kivaisi AK. The potential for constructed wetlands for wastewater treatment and reuse in developing countries: a review. Ecological Engineering 2001;16:545–60.
[3] Wilkie AC, Evans JM. Aquatic plants: an opportunity feedstock in the age of bioenergy. Biofuels 2010;1:311–21.
[4] Harley KLS. The role of biological control in the management of water hyacinth, *Eichhornia crassipes*. Biocontrol News and Information 1990;11:11–22.
[5] Malik A. Environmental challenge vis a vis opportunity: the case of water hyacinth. Environment International 2007;33:122–38.
[6] Gopal B, Sharma KP. Water-hyacinth (*Eichhornia crassipes*) the most troublesome weed of the world 1981.
[7] Kumar S, Kothari U, Kong L, Lee YY, Gupta RB. Hydrothermal pretreatment of switchgrass and corn stover for production of ethanol and carbon microspheres. Biomass and Bioenergy 2011;35:956–68.
[8] Peterson AA, Vogel F, Lachance RP, Froling M, Antal JMJ, Tester JW. Thermochemical biofuel production in hydrothermal media: a review of sub- and supercritical water technologies. Energy & Environmental Science 2008;1:32–65.
[9] Sevilla M, Fuertes AB. The production of carbon materials by hydrothermal carbonization of cellulose. Carbon 2009;47:2281–9.
[10] Sevilla M, Fuertes AB. Chemical and structural properties of carbonaceous products obtained by hydrothermal carbonization of saccharides. Chemistry–A European Journal 2009;15:4195–203.
[11] Erlach B, Harder B, Tsatsaronis G. Combined hydrothermal carbonization and gasification of biomass with carbon capture. Energy 2012;45:329–38.
[12] Gunnarsson CC, Petersen CM. Water hyacinths as a resource in agriculture and energy production: a literature review. Waste Management 2007;27:117–29.
[13] Biller P, Ross AB. Hydrothermal processing of algal biomass for the production of biofuels and chemicals. Biofuels 2012;3:603–23.
[14] Ong YK, Bhatia S. The current status and perspectives of biofuel production via catalytic cracking of edible and non-edible oils. Energy 2010;35:111–9.
[15] Gurung A, Van Ginkel SW, Kang W-C, Qambrani NA, Oh S-E. Evaluation of marine biomass as a source of methane in batch tests: a lab-scale study. Energy 2012.
[16] Nigam JN. Bioconversion of water-hyacinth (*Eichhornia crassipes*) hemicellulose acid hydrolysate to motor fuel ethanol by xylose-fermenting yeast. Journal of Biotechnology 2002;97:107–16.
[17] Kurniati A, Darmokoesoemo H, Puspaningsih NNT. Modification of surface structure and crystallinity of water hyacinth (*Eichhornia crassipes*) following recombinant α-L-arabinofuranosidase (abfa) treatment. Journal of Agricultural Biotechnology and Sustainable Development 2011;3:182–8.
[18] Mishima D, Kuniki M, Sei K, Soda S, Ike M, Fujita M. Ethanol production from candidate energy crops: water hyacinth (*Eichhornia crassipes*) and water lettuce (*Pistia stratiotes* L.). Bioresource Technology 2008;99:2495–500.
[19] Xia A, Cheng J, Lin R, Ding L, Zhou J, Cen K. Combination of hydrogen fermentation and methanogenesis to enhance energy conversion efficiency from trehalose. Energy 2013.
[20] Tekin K, Karagöz S. Non-catalytic and catalytic hydrothermal liquefaction of biomass. Research on Chemical Intermediates 2012:1–14.
[21] Toor SS, Rosendahl L, Rudolf A. Hydrothermal liquefaction of biomass: a review of subcritical water technologies. Energy 2011;36:2328–42.
[22] Huang H-j, Yuan X-z, Zhu H-n, Li H, Liu Y, Wang X-l, et al. Comparative studies of thermochemical liquefaction characteristics of microalgae, lignocellulosic biomass and sewage sludge. Energy 2013.
[23] Kruse A. Hydrothermal biomass gasification. The Journal of Supercritical Fluids 2009;47:391–9.
[24] Singhal V, Rai JPN. Biogas production from water hyacinth and channel grass used for phytoremediation of industrial effluents. Bioresource Technology 2003;86:221–5.
[25] Elliott DC, Sealock LJ, Butner RS. Product analysis from direct liquefaction of several high-moisture biomass feedstocks. Pyrolysis Oils from Biomass, American Chemical Society 1988;376:179–88.
[26] Gao Y, Chen H-p, Wang J, Shi T, Yang H-P, Wang X-H. Characterization of products from hydrothermal liquefaction and carbonation of biomass model compounds and real biomass. Journal of Fuel Chemistry and Technology 2011;39:893–900.
[27] Gao Y, Wang X, Yang H, Chen H. Characterization of products from hydrothermal treatments of cellulose. Energy 2012;42:457–65.

[28] Ghetti P, Ricca L, Angelini L. Thermal analysis of biomass and corresponding pyrolysis products. Fuel 1996;75:565–73.
[29] Harun MY, Dayang Radiah AB, Zainal Abidin Z, Yunus R. Effect of physical pretreatment on dilute acid hydrolysis of water hyacinth (*Eichhornia crassipes*). Bioresource Technology 2011;102:5193–9.
[30] Krevelen DWV. Graphical-statistical method for the study of structure and reaction processes of coal. Fuel 1950;24:269–84.
[31] Williams A, Jones JM, Ma L, Pourkashanian M. Pollutants from the combustion of solid biomass fuels. Progress in Energy and Combustion Science 2012;38:113–37.
[32] Wang Q, Li H, Chen L, Huang X. Novel spherical microporous carbon as anode material for Li-ion batteries. Solid State Ionics 2002;152–153:43–50.
[33] Kumar S, Gupta RB. Biocrude production from switchgrass using subcritical water. Energy & Fuels 2009;23:5151–9.
[34] Chen Y, Yang H, Wang X, Zhang S, Chen H. Biomass-based pyrolytic polygeneration system on cotton stalk pyrolysis: influence of temperature. Bioresource Technology 2012;107:411–8.
[35] Maeda RN, Serpa VI, Rocha VAL, Mesquita RAA, Anna LMMS, de Castro AM, et al. Enzymatic hydrolysis of pretreated sugar cane bagasse using *Penicillium funiculosum* and *Trichoderma harzianum* cellulases. Process Biochemistry 2011;46:1196–201.
[36] Nishimiya K, Hata T, Imamura Y, Ishihara S. Analysis of chemical structure of wood charcoal by X-ray photoelectron spectroscopy. Journal of Wood Science 1998;44:56–61.
[37] Wu B, Hu H, Zhao Y, Jin L, Fang Y. XPS analysis and combustibility of residues from two coals extraction with sub- and supercritical water. Journal of Fuel Chemistry and Technology 2009;37:385–92.